

**NANO EXPRESS**

**Open Access**

# Quantum dot/glycol chitosan fluorescent nanoconjugates

Alexandra AP Mansur and Herman S Mansur\*

## Abstract

In this study, novel carbohydrate-based nanoconjugates combining chemically modified chitosan with semiconductor quantum dots (QDs) were designed and synthesised via single-step aqueous route at room temperature. Glycol chitosan (G-CHI) was used as the capping ligand aiming to improve the water solubility of the nanoconjugates to produce stable and biocompatible colloidal systems. UV-visible (UV-vis) spectroscopy, photoluminescence (PL) spectroscopy, and Fourier transform infrared (FTIR) spectroscopy were used to characterise the synthesis and the relative stability of biopolymer-capped semiconductor nanocrystals. The results clearly demonstrated that the glycol chitosan derivative was remarkably effective at nucleating and stabilising semiconductor CdS quantum dots in aqueous suspensions under acidic, neutral, and alkaline media with an average size of approximately 2.5 nm and a fluorescent activity in the visible range of the spectra.

**PACS:** 81.07.Ta; 78.67.Hc; 82.35.Pq

**Keywords:** Glycol chitosan; Nanoparticle; Quantum dot; Colloid; Biopolymer; Bioconjugates; Nanomaterials

## Background

Approximately 3 decades ago, quantum dots (QDs) emerged as a notable class of nanomaterials because of their unique set of optical, electronic, magnetic, and chemical properties [1-3]. Essentially, QDs are ultra-small semiconductor crystalline nanoparticles with size-dependent properties, which possess higher luminescence, narrower emission band, broader excitation wavelength range, and greater photostability compared with fluorescent organic dyes [2]. Due to their small dimensions with extremely high surface area, these fluorescent nanocrystals must be stabilised by capping agents during their synthesis to restrict the growth of the nucleated nanoparticles [4]. Thus, QDs have been produced using a myriad of processes, such as entrapment in molecular films [5,6] and glasses [7,8], as well as encapsulation in polymer nanoparticles [9], organic solvents [10], and colloidal dispersions [11].

Since the seminal work of Murray et al. [12], the majority of QDs have been developed using organometallic

routes at high temperature because they commonly result on monodisperse nanoparticles with high luminescent behaviour. However, water-soluble QDs have increasingly attracted the attention of the research community based on their potential use in biomedical and environmentally friendly applications [1,13,14]. Therefore, water-soluble polymers are a promising platform to develop innovative QD nanohybrids because they offer an attractive set of physicochemical properties associated with broad availability, large variety of chemical structures at relative low cost. In addition, polymers can be chemically functionalised and conjugated with other molecules for designed and specific applications [15-17]. Among the numerous alternative polymers for biomedical applications, chitosan (CHI) and its derivatives have often been selected due to their multidimensional properties [18,19]. However, chitosan is reasonably water-soluble only under acidic conditions, and it is practically insoluble at neutral and alkaline pH (at pH higher than its pKa ~ 6.5), which significantly restricts its applications in medicine and biology at physiological pH (approximately 7.4). Hence, the chemical modifications of chitosan for producing water-soluble derivatives in a broader pH range, mainly under physiological conditions, are highly attractive for the preparation of nanohybrids and nanoconjugates for

\* Correspondence: hmansur@demet.ufmg.br  
Center of Nanoscience, Nanotechnology and Innovation - CeNano21,  
Department of Metallurgical and Materials Engineering, Federal University of  
Minas Gerais, Av. Antônio Carlos, 6627 - Escola de Engenharia, Bloco 2 - Sala  
2233, Belo Horizonte, MG 31.270-901, Brazil

nanomedicine [9,20-25]. Surprisingly, only few reports have been published in the literature using chitosan and its derivatives as direct capping ligands for the synthesis of QDs in aqueous media [21-24].

Glycol chitosan (G-CHI) is a commercially available derivate of chitosan with improved hydrophilicity and biocompatibility and is frequently used in various biomedical applications such as drug delivery, siRNA carrier, cancer imaging, and therapy [26]. Interesting reports using G-CHI combined with nanomaterials (e.g. gold nanoparticles) have been published by Kim and collaborators [26,27], as well as studies on PEG-conjugated chitosan derivatives for the preparation of QDs [28]. Nevertheless, no study was found in the consulted literature addressing the direct synthesis of QDs using glycol chitosan as capping ligands by aqueous colloidal chemistry.

Thus, in this study, novel carbohydrate-based nanoconjugates combining glycol chitosan with CdS semiconductor QDs were designed and synthesised via a single-step aqueous process at room temperature. G-CHI was used as the capping ligand to produce water-soluble colloidal bioconjugates. The results demonstrated that the glycol chitosan derivative was effective at nucleating and stabilising luminescent CdS QDs in aqueous colloidal dispersions under acidic, physiological, and alkaline media, indicating considerable potential for biomedical and pharmaceutical applications in nanomedicine.

## Methods

### Materials

All of the reagents and precursors, including cadmium perchlorate hydrate (Sigma-Aldrich, St. Louis, MO, USA,  $\text{Cd}(\text{ClO}_4)_2 \cdot 6\text{H}_2\text{O}$ ), sodium sulphide (Synth, Diadema, Brazil, >98%,  $\text{Na}_2\text{S} \cdot 9\text{H}_2\text{O}$ ), and hydrochloric acid (Sigma-Aldrich, St. Louis, MO, USA, 36.5% to 38%, HCl) were used as received. Glycol chitosan (G-CHI; Sigma-Aldrich, St. Louis, MO, USA, PN# G7753; degree of polymerization  $\geq 400$ , lot supplied = 2,000 ( $M_w \sim 410$  kDa); degree of deacetylation DD  $\geq 60\%$ , lot supplied = 76.2%) was used as the ligand. Chitosan (Aldrich Chemical, St. Louis, MO, USA, catalogue#419419; high molecular weight,  $M_w = 310$  to  $>395$  kDa; degree of deacetylation DD  $\geq 75.0\%$ ; viscosity 800 to 2,000 cPoise, 1 wt.% in 1% acetic acid) was used as the reference polysaccharide ligand. Unless otherwise indicated, deionised water (DI water; Millipore Simplicity™, Millipore, Billerica, MA, USA) with a resistivity of  $18 \text{ M}\Omega \cdot \text{cm}$  was used to prepare the solutions, and the procedures were conducted at room temperature (RT;  $23^\circ\text{C} \pm 2^\circ\text{C}$ ).

### Synthesis of CdS quantum dots

A chitosan solution (1%, *w/v*) was prepared by dispersing CHI powder in an aqueous solution (2%, *v/v*) of acetic

acid. The mixture was placed under constant stirring overnight at room temperature, until complete solubilisation had occurred ( $\text{pH} \sim 3.6$ ). Glycol chitosan solution (1.0%, *w/v*) was prepared by dissolving G-CHI powder in DI water under moderate magnetic stirring for 2 h until complete solubilisation had occurred ( $\text{pH} \sim 8.4$ ). Before synthesising the CdS QDs, chitosan and glycol chitosan solutions were diluted with DI water to a concentration of  $0.4 \text{ mg}\cdot\text{mL}^{-1}$  and the pH was adjusted with NaOH or HCl solutions ( $0.1 \text{ mol}\cdot\text{L}^{-1}$ ). CdS nanoparticles stabilised by G-CHI and CHI were synthesised via an aqueous route in a reaction flask at room temperature as previously described [29]: glycol chitosan solution or chitosan solution ( $0.4 \text{ mg}\cdot\text{mL}^{-1}$ ) was added to the flask. With moderate magnetic stirring, the  $\text{Cd}^{2+}$  ( $\text{Cd}(\text{ClO}_4)_2 \cdot 6\text{H}_2\text{O}$ ,  $0.75 \text{ mmol}\cdot\text{L}^{-1}$ ) and  $\text{S}^{2-}$  precursor solutions ( $\text{Na}_2\text{S} \cdot 9\text{H}_2\text{O}$ ,  $0.37 \text{ mmol}\cdot\text{L}^{-1}$ ) were added to the reaction flask (S:Cd molar ratio was kept at 1:2) and stirred for 3 min. The obtained CdS QD dispersions were clear, homogeneous, and yellowish, which were referred to as CdS\_G-CHI\_5.0, CdS\_G-CHI\_7.4, CdS\_G-CHI\_8.4, and CdS\_CHI\_6.0 based on the capping ligand and pH used during the synthesis ( $5.0 \pm 0.2$ ,  $7.4 \pm 0.2$ ,  $8.4 \pm 0.2$ , and  $6.0 \pm 0.2$ , respectively). The CdS QD colloids were dialyzed for 24 h (water changes after 2 and 4 h) against 3 L of DI water using a cellulose membrane with molecular weight cutoff (MWCO) of 14,000 Da with moderate stirring at room temperature. After purification, the QD dispersions were stored at  $6^\circ\text{C} \pm 2^\circ\text{C}$  for further use.

### Characterisation of the CdS quantum dots and capping agents

UV-visible (UV-vis) spectroscopy measurements were conducted using a PerkinElmer instrument (Lambda EZ-210, PerkinElmer, Waltham, MA, USA) in the transmission mode with samples in a quartz cuvette over a wavelength range of 600 to 190 nm. All of the experiments were conducted in triplicates ( $n = 3$ ) unless specifically noted, and the data are presented as the mean  $\pm$  standard deviation.

Photoluminescence (PL) characterisation of the CdS conjugates was conducted based on spectra acquired at room temperature using a violet diode laser module at  $\lambda_{\text{exc}} = 405 \text{ nm}$  (150 mW, Roithner LaserTechnik, GmbH, Vienna, Austria) coupled to a USB4000 VIS-NIR spectrophotometer (Ocean Optics, Dunedin, FL, USA). All of the tests were performed using a minimum of four repetitions ( $n \geq 4$ ). Digital colour images were collected of the QD fluorescence in the visible range of the spectrum (cutoff filter 535 nm).

Nanostructural characterisations of the QD bioconjugates were based on the images and selected area

electron diffraction (SAED) patterns obtained using a Tecnai G2-20-FEI transmission electron microscope (TEM; FEI, Hillsboro, OR, USA) at an accelerating voltage of 200 kV. Energy-dispersive X-ray (EDX) spectra were collected using the TEM for element chemical analysis. In all of the TEM analyses, the samples were prepared by dropping the colloidal dispersion onto a porous carbon grid. The QD size and size-distribution data were obtained based on the TEM images by measuring at least 100 randomly selected nanoparticles using an image processing program (ImageJ, version 1.44, public domain, National Institutes of Health).

X-ray diffraction (XRD) patterns were recorded using a PANalytical X'Pert diffractometer (PANalytical, Almelo, The Netherlands) (Cu-K $\alpha$  radiation with  $\lambda = 1.5406 \text{ \AA}$ ). Measurements were performed in the  $2\theta$  range from  $6^\circ$  to  $70^\circ$  with steps of  $0.067^\circ$ . For sample preparation, QD colloidal medium was concentrated and purified using an Amicon<sup>®</sup> Ultra Filter (Millipore, Billerica, MA, USA) with a 30,000 molecular mass ( $M_w$ ) cutoff cellulose membrane, dropped on a glass slide and dried in an oven at  $40^\circ\text{C} \pm 1^\circ\text{C}$  for 12 h.

Dynamic light scattering (DLS) and Zeta potential (ZP) analyses were performed using a Brookhaven ZetaPlus instrument (Brookhaven Instruments Corporation, Holtsville, NY, USA) with a laser light with wavelength of 660 nm (35-mW red diode laser) and a thermostat with temperature stabilisation. Standard square acrylic cells with a volume of 4.5 mL were used. Samples were measured at the temperature of  $25^\circ\text{C} \pm 2^\circ\text{C}$ , and the light scattering was detected at the angle of  $90^\circ$ . Before the DLS analysis of the QDs, the colloidal solutions (3 mL) were filtered three times through a  $0.45\text{-}\mu\text{m}$  aqueous syringe filter (Millex LCR 25 mm, Millipore, Billerica, MA, USA) to remove any possible dust. Five measurements were obtained for each system and averaged. Zeta potential measurements were performed in the CdS QD colloidal aqueous solutions using the laser Doppler electrophoresis technique. All of the tests were performed using a minimum of ten replicates ( $n \geq 10$ ), and the values were averaged.

CdS quantum dots and ligands were analysed by the diffuse reflectance infrared Fourier transform spectroscopy (DRIFTS) method (Thermo Fisher Scientific, Waltham, MA, USA, Nicolet 6700) over the range from  $4,000$  to  $400 \text{ cm}^{-1}$  using 64 scans and a  $4 \text{ cm}^{-1}$  resolution. These samples were prepared by placing a droplet of the G-CHI solution, CHI solution, or CdS QD dispersions onto KBr powder and drying at  $60^\circ\text{C} \pm 2^\circ\text{C}$  for 24 h. Glycol chitosan as supplied was also pressed and analysed by attenuated total reflectance (ATR) over the range of  $4,000$  to  $675 \text{ cm}^{-1}$  using 32 scans and a  $4 \text{ cm}^{-1}$  resolution.

## Results and discussion

### Characterisation of CdS quantum dots capped by chitosan

#### UV-vis spectroscopy

Figure 1A presents the UV-vis spectroscopy results from the synthesis of semiconductor nanoparticles using glycol chitosan at physiological pH (7.4) as the stabilising ligand compared with chitosan. The pH of 6.0 was selected for the synthesis of the quantum dots with chitosan because this polymer is water-soluble at pH values lower than approximately 6.0 [30]. Under acidic conditions, the amine groups of chitosan are partially or completely protonated, resulting in the repulsion between chains, thereby favouring the chitosan-water interaction, which overcomes the associative forces between chains and promotes chitosan solubility.

The UV-vis absorption spectra of the CdS nanoconjugates exhibit a broad absorption band between 300 to 450 nm associated with the first excitonic transition ( $\lambda_{\text{exc}}$ ). This result indicates that CdS nanocrystals were synthesised within the 'quantum confinement regime'

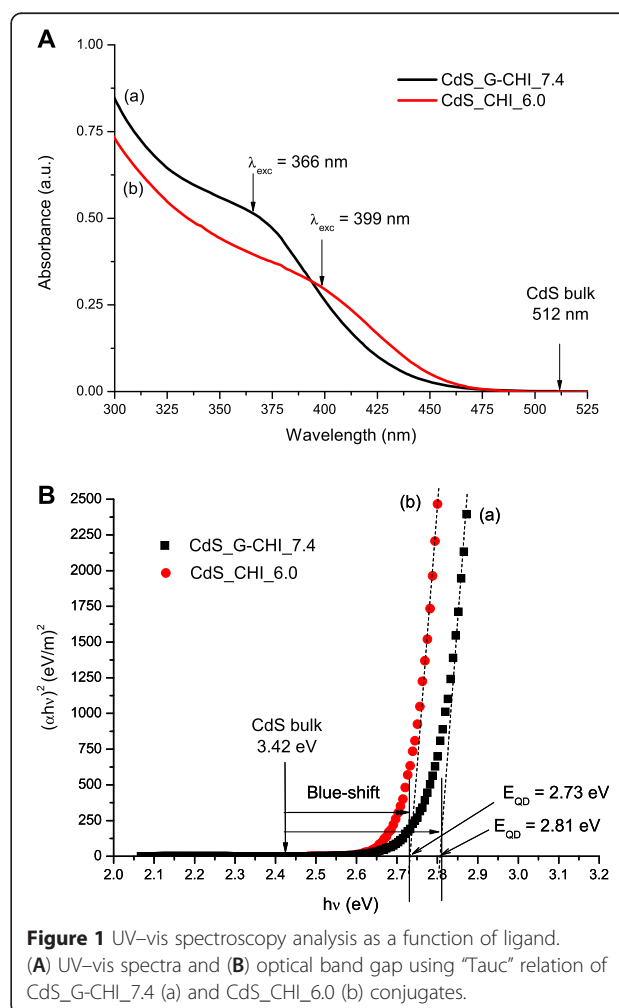


**Figure 1** UV-vis spectroscopy analysis as a function of ligand. (A) UV-vis spectra and (B) optical band gap using "Tauc" relation of CdS\_G-CHI\_7.4 (a) and CdS\_CHI\_6.0 (b) conjugates.

based on the energy blueshift observed for the curves compared with the 'bulk' value for the CdS semiconductor (Figure 1A, arrow at  $\lambda = 512$  nm) [1]. The average sizes of CdS nanoparticles were determined using Henglein's empirical model [31], which relates the diameter of the CdS nanoparticle ( $2R$ ) to the exciton absorption transition onset ( $\lambda_{exc}$ ) in the UV-vis spectra according to Equation 1.

$$2R(\text{nm}) = \frac{0.1}{0.1338 - 0.0002345 * \lambda_{exc}} \quad (1)$$

Based on the UV-vis spectra, the average sizes (diameter,  $2R$ ) were calculated as  $2.1 \pm 0.1$  and  $2.5 \pm 0.1$  nm for CdS\_G-CHI\_7.4 and CdS\_CHI\_6.0, respectively.

The optical band gap (absorbance onset,  $E_{QD}$ ) values of QDs extracted from the curves using the 'Tauc relation' [32] (Figure 1B) were  $2.81 \pm 0.02$  and  $2.73 \pm 0.02$  eV for QDs stabilised by glycol chitosan and chitosan, respectively. Because these band gap values ( $E_{QD}$ ) are higher than the reference bulk value ( $E_g = 2.42$  eV) for CdS referred to as "blueshift" (i.e.  $E_{QD} - E_g$ ), it can be stated that colloidal CdS QDs were effectively synthesised in aqueous media using glycol chitosan ligands at physiological conditions. To the best of our knowledge, there has been no reported literature in which bioconjugates based on CdS QDs were directly produced and stabilised by glycol chitosan as the capping ligand that were synthesised at room temperature using strictly water colloidal chemistry.

The UV-vis results presented in Figure 2 also demonstrated that the glycol chitosan derivative was effective at nucleating and stabilising CdS QDs in aqueous suspensions in acidic (Figure 2(c), CdS\_G-CHI\_5.0), neutral

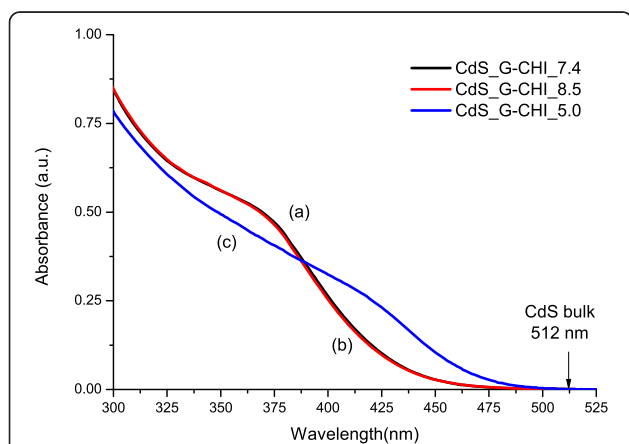


**Figure 2** UV-vis spectroscopy analysis as a function of pH. UV-vis spectra for CdS\_G-CHI\_7.4 (a), CdS\_G-CHI\_8.5 (b), and CdS\_G-CHI\_5.0 (c).

(Figure 2(a), CdS\_G-CHI\_7.4), and alkaline (Figure 2(b), CdS\_G-CHI\_8.4) media.

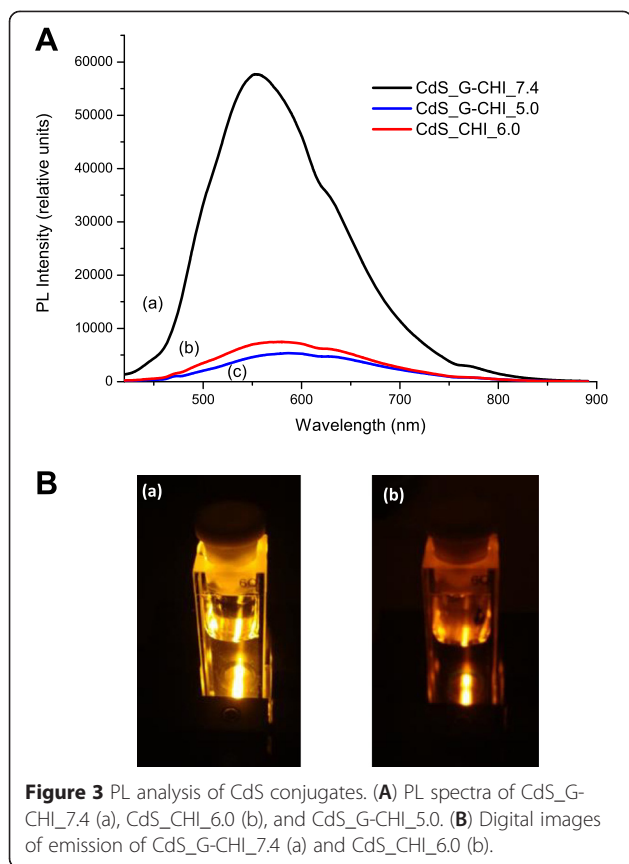
Based on the spectra in Figure 2 and the results presented in Table 1, the pH significantly influences the formation/growth/stabilisation of the CdS QDs in the glycol chitosan colloidal solution. When the synthesis pH was raised from acidic to neutral and then alkaline, the nanocrystal size decreased. At pH = 5.0, some of the amine groups of glycol chitosan are protonated, forcing the positively charged transition metal to compete with a hydrogen ion for complexation with an amine electron pair (metal-ligand interactions). However, as the pH increases to 7.4 and 8.5, most of the amine groups in the glycol chitosan chain become available for dative bonding (electron donor) with  $\text{Cd}^{2+}$ , thus reducing the electrostatic repulsion ( $\text{Cd}^{2+} \leftrightarrow \text{NH}_3^+$ ) and favouring the stabilisation of the CdS nanocrystals at smaller dimensions. The similarity of the QD parameters ( $\lambda_{exc}$ ,  $2R$ , and  $E_{QD}$ ) measured in neutral and alkaline media indicates that the amine groups of G-CHI are fully deprotonated at pH 7.4 (pKa ~ 6.5).

#### Photoluminescence spectroscopy analysis

Figure 3A shows the photoluminescence spectra of the nano hybrids synthesised with glycol chitosan (pH = 7.4

**Table 1** Quantum dots parameters: excitonic transition wavelength, estimated particle diameter, band-gap energy, and blueshift

System	Ligand	pH	Parameter	Values
CdS_G-CHI_7.4	Glycol chitosan	7.4 ± 0.2	$\lambda_{exc}$ (nm)	369 ± 2
			$2R$ (nm)	2.1 ± 0.1
			(CdS) ( $\mu\text{mol.L}^{-1}$ )	4.4 ± 0.2
			$E_{QD}$ (eV)	2.81 ± 0.02
			Blueshift (eV)	0.39 ± 0.02
CdS_G-CHI_5.0	Glycol chitosan	5.0 ± 0.2	$\lambda_{exc}$ (nm)	413 ± 2
			$2R$ (nm)	2.7 ± 0.1
			(CdS) ( $\mu\text{mol.L}^{-1}$ )	1.3 ± 0.2
			$E_{QD}$ (eV)	2.64 ± 0.02
			Blueshift (eV)	0.22 ± 0.02
CdS_G-CHI_8.5	Glycol chitosan	8.5 ± 0.2	$\lambda_{exc}$ (nm)	367 ± 2
			$2R$ (nm)	2.1 ± 0.1
			(CdS) ( $\mu\text{mol.L}^{-1}$ )	4.4 ± 0.2
			$E_{QD}$ (eV)	2.81 ± 0.02
			Blueshift (eV)	0.39 ± 0.02
CdS_CHI_6.0	Chitosan	6.0 ± 0.2	$\lambda_{exc}$ (nm)	399 ± 2
			$2R$ (nm)	2.5 ± 0.1
			(CdS) ( $\mu\text{mol.L}^{-1}$ )	1.8 ± 0.2
			$E_{QD}$ (eV)	2.73 ± 0.02
			Blueshift (eV)	0.31 ± 0.02



and pH = 5.0, Figure 3A(a) and Figure 3A(c) and chitosan (pH = 6.0, Figure 3A(b)) collected at room temperature. The band edge (excitonic) emission was not detected, and the emissions in the green-red range arising from the intrinsic defects in the nanocrystals were observed for both of the systems, as reported in the literature [15,16,21,33–35]. The green luminescence is favoured by the synthesis of nanoparticles under an excess of metal cations ( $\text{Cd}^{2+}$ ) [33–35], compatible with the procedure used in this study [29] (molar ratio of cation: anion = 2:1). The orange luminescence arises from the interstitial atoms of the metal in the semiconductor lattice ( $\text{Cd}_i$ ), while the red band of PL is assigned to vacancy states ( $V_{\text{Cd}} - V_{\text{S}}$  or  $V_{\text{S}}$ ) [34,35]. In addition, note that the luminescent response of G-CHI QDs nanoparticles was approximately 7.5-fold higher than the measured value for CdS\_CHI\_6.0 system (Figure 3A). This behaviour can be qualitatively observed in the images showed in Figure 3B with the much stronger luminescent response of G-CHI QDs nanoparticles (image, a) compared to CHI QDs (image, b). As luminescence is directly proportional to nanoparticles concentration, it was expected that the emission of the CdS\_G-CHI\_7.4 system would be more intense compared with CdS\_CHI\_6.0 because the molar concentration of glycol QDs is approximately 2.5 times higher (Table 1). In contrast,

because glycol chitosan nanoparticles were 20% smaller than chitosan stabilised nanocrystals, it is considered that the higher surface disorder, under-coordinated sites, and dangling bonds would dominate the luminescent properties, thus creating non-radiative pathways that dissipate quantum dot emissions, which resulted in the decreased PL intensity. The overall balance is an increased luminescence intensity that may also be favoured by the absence of protonated amines at pH 7.4 that can act as electron scavengers, quenching the photoluminescence. For the CdS\_G-CHI\_5.0 nanoconjugates, the intensity of the PL spectrum was relatively lower than the response from the CdS\_CHI\_6.0 sample, which was assigned to the higher number of protonated amine groups at lower pH, as the sizes of both nanoparticles were equivalent.

#### TEM morphological analysis

In this study, the morphological and structural features of the CdS QDs were characterised using transmission electron microscopy (TEM) coupled to an EDX microprobe and using SAED analysis. Figure 4A shows a representative image of CdS QDs produced with glycol chitosan as the capping agent at pH = 7.4. Some of the CdS\_G-CHI\_7.4 nanoparticles are clustered, but the isolated particles showed an apparent spherical morphological feature. Figure 4B shows the SAED pattern of the CdS nanoparticles indicating that nanoparticles were crystalline in nature. The histogram of the CdS\_G-CHI\_7.4 size distribution (Figure 4D) indicates a relatively monodisperse distribution with an average size of  $2.5 \pm 0.3$  nm in agreement with the values estimated by UV–vis spectroscopy in the previous sections ( $2R = 2.1 \pm 0.1$  nm). EDX spectrum shows the chemical analysis of the nanocrystals with Cd and S as the major elements (Figure 4C), excluding copper, oxygen, and carbon peaks related to the TEM grid and the polymer stabiliser, and Si from the detector. Thus, the TEM results demonstrated that the CdS QDs were properly stabilised by glycol chitosan under physiological conditions.

#### XRD analysis

The XRD pattern of the CdS\_G-CHI\_7.4 nanoconjugates (Figure 4E) presented a broad peak in the range of  $20^\circ$  to  $25^\circ$  associated with the semicrystalline structure of the polymer capping agent and four peaks centred at  $2\theta$   $26.2^\circ$  ( $d = 0.34$  nm),  $30.3^\circ$  ( $d = 0.29$  nm),  $43.9^\circ$  ( $d = 0.21$  nm), and  $51.9^\circ$  ( $d = 0.18$  nm), which can be attributed to CdS with cubic lattice structure (JCPDS 89–0440). Some peak broadening in the XRD pattern is normally observed caused by the formation of ultra-small nanocrystals, i.e. CdS quantum dots, combined with overlapped scattering from the biopolymer ligands. These results were compatible with the lattice fringes of

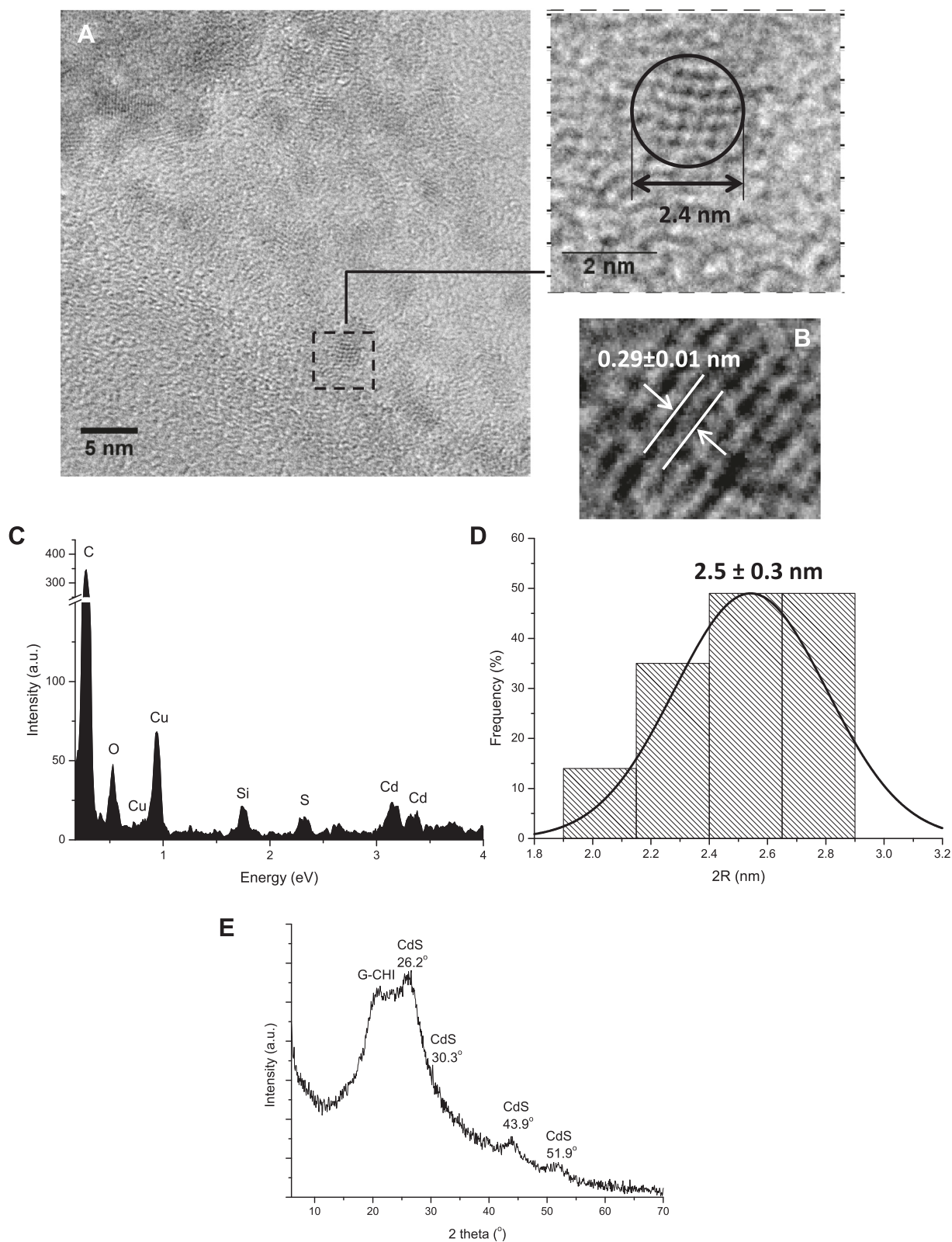


**Figure 4** Morphological and structural analysis of CdS\_G-CHI\_7.4. **(A)** TEM image. **(B)** Nanocrystal plane spacing (SAED). **(C)** EDX spectrum. **(D)** Histogram of nanoparticle size distribution. **(E)** X-ray diffraction pattern.

an inter-planar distance of approximately  $0.29 \pm 0.01$  nm assigned to the (200) plane and revealed by the SAED pattern (Figure 4B).

#### DLS and ZP analyses

The DLS results showed that the 'number-average' diameters of CdS\_G-CHI\_7.4 and CdS\_CHI\_6.0 were  $40.4 \pm 3.3$  and  $16.6 \pm 0.6$  nm, respectively. These values are higher than the semiconductor nanoparticle sizes estimated using the UV-vis absorbance curves and TEM analysis (2.1 to 2.5 nm). This trend was expected because DLS values correspond to the 'hydrodynamic diameter' (*HD*) of the nanoconjugates in the colloidal media and include the organic shell (capping ligand) and the inorganic core (CdS nanocrystal), and they cannot be directly compared to the TEM results ('dry' morphological analysis) or the UV-vis measurements (energy of band gap absorption). The difference of dimensions between the conjugates stabilised by CHI and G-CHI is mostly associated with the capping ligand, and they can be explained based on the influence of the solvation layers and polyelectrolyte effects. At pH = 6.0 (CdS\_CHI\_6.0), hydrogen bonds and hydrophobic interactions between chitosan chains are more favourable once the number of  $-\text{NH}_3^+$  species and the interchain repulsive electrostatic forces are reduced, promoting the formation of a more compact structure. On the other hand, the more hydrophilic ethylene glycol groups grafted to the chitosan derivative present higher interaction with aqueous medium with a consequent enlargement of the organic shell of the nanosystem measured by the *HD* values in the DLS assays.

The ZP values ( $\zeta$ ) of CdS\_CHI\_6.0 conjugates were almost neutral ( $0.0 \pm 0.5$  mV) indicating that the surface of these nanoparticles was mainly covered with CHI polymer. The surface charge of chitosan tends towards zero at pH values near the isoelectric point of chitosan (i.e. pH from 6.0 to 7.0), in agreement with the compact structure evaluated by the DLS assay. The positive values of ZP for CdS\_G-CHI\_7.4 nanoconjugates ( $+9.9 \pm 3.3$  mV) were influenced by the inorganic nanoparticle surface charge, which was expected to be positive as a result of the synthesis performed under the excess of cadmium cations, associated with the more 'open' structure of glycol chitosan shell. In addition, because the ZP results were above  $-30$  mV and below  $+30$  mV, CdS nanoconjugates were not predominantly stabilised by electrostatic balance but relied on the steric hindrance of the polymer shell to prevent close contact between the nanoparticles.

#### FTIR spectroscopy analysis

The FTIR spectra of glycol chitosan as supplied and of glycol chitosan (pH =  $7.4 \pm 0.2$ ) and chitosan (pH =  $6.0 \pm$

0.2) after solubilisation are shown in Figure 5. The FTIR spectrum of chitosan presented absorption peaks at  $3,400$  to  $3,200$   $\text{cm}^{-1}$  (OH stretching overlapped with NH stretching),  $3,000$  to  $2,800$   $\text{cm}^{-1}$  (CH stretching),  $1,650$  to  $1,640$   $\text{cm}^{-1}$  (C=O stretching amide I),  $1,590$  to  $1,560$   $\text{cm}^{-1}$  (NH bending, primary amine and amide II), and  $1,450$  to  $1,380$   $\text{cm}^{-1}$  (CH bending). In addition, the absorptions at  $1,020$  to  $1,050$   $\text{cm}^{-1}$  and  $1,070$  to  $1,110$   $\text{cm}^{-1}$  indicate the C-O stretching vibrations in chitosan, which are associated with the C6-OH primary alcohol and the C3-OH secondary alcohol, respectively, and the bands at  $1,160$  and  $996$   $\text{cm}^{-1}$  are assigned to the vibrations of the C-O-C saccharide bridge [36]. The modification of chitosan with the ethylene glycol (EG) moiety introduced chemical groups in the polymer chain (G-CHI) such as ether (C-O-C,  $1,150$  to  $1,050$   $\text{cm}^{-1}$ ), alcohol ( $-\text{C}-\text{O}$ ,  $1,260$  to  $1,000$   $\text{cm}^{-1}$ ), alkane (CH,  $2,960$  to  $2,850$   $\text{cm}^{-1}$  and  $1,450$  to  $1,300$   $\text{cm}^{-1}$ ), and hydroxyl (OH,  $3,600$  to  $3,200$   $\text{cm}^{-1}$ ) [37,38], which mostly overlap the chitosan absorption bands. In addition to these bands, in the spectrum of the as-supplied glycol chitosan, the vibrations at  $945$  and  $892$   $\text{cm}^{-1}$ , associated with  $-\text{CH}_2$  rocking [37] and the  $-\text{OC}_2\text{H}_4$  backbone [38], respectively, were observed. Note that the primary amine band of the as-supplied glycol chitosan was shifted from  $1,560$  to  $1,590$   $\text{cm}^{-1}$  compared with chitosan. After solubilisation of glycol chitosan, this shift was higher, from  $1,560$  to  $1,618$   $\text{cm}^{-1}$  [39]. These shifts are related to the interactions between the hydrophilic OH groups from the EG moiety and NH from the primary amines of chitosan through hydrogen bonds.

After conjugating the quantum dots with the capping glycol chitosan biopolymer (curves (b) in Figure 6), several bands of G-CHI were observed in the FTIR spectra (curves (a) in Figure 6) that exhibited changes in their energies (i.e., wavenumber). These changes can be

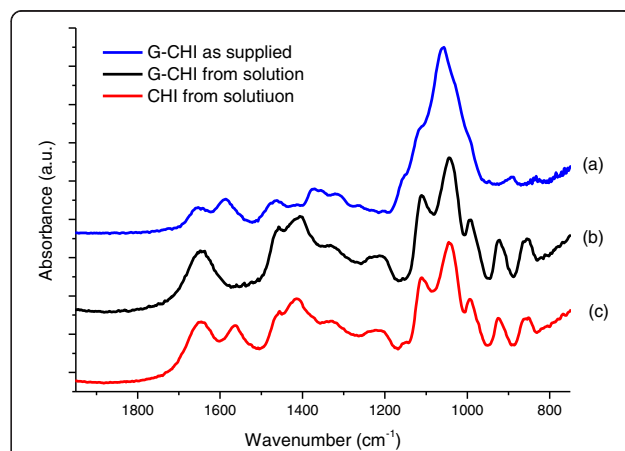
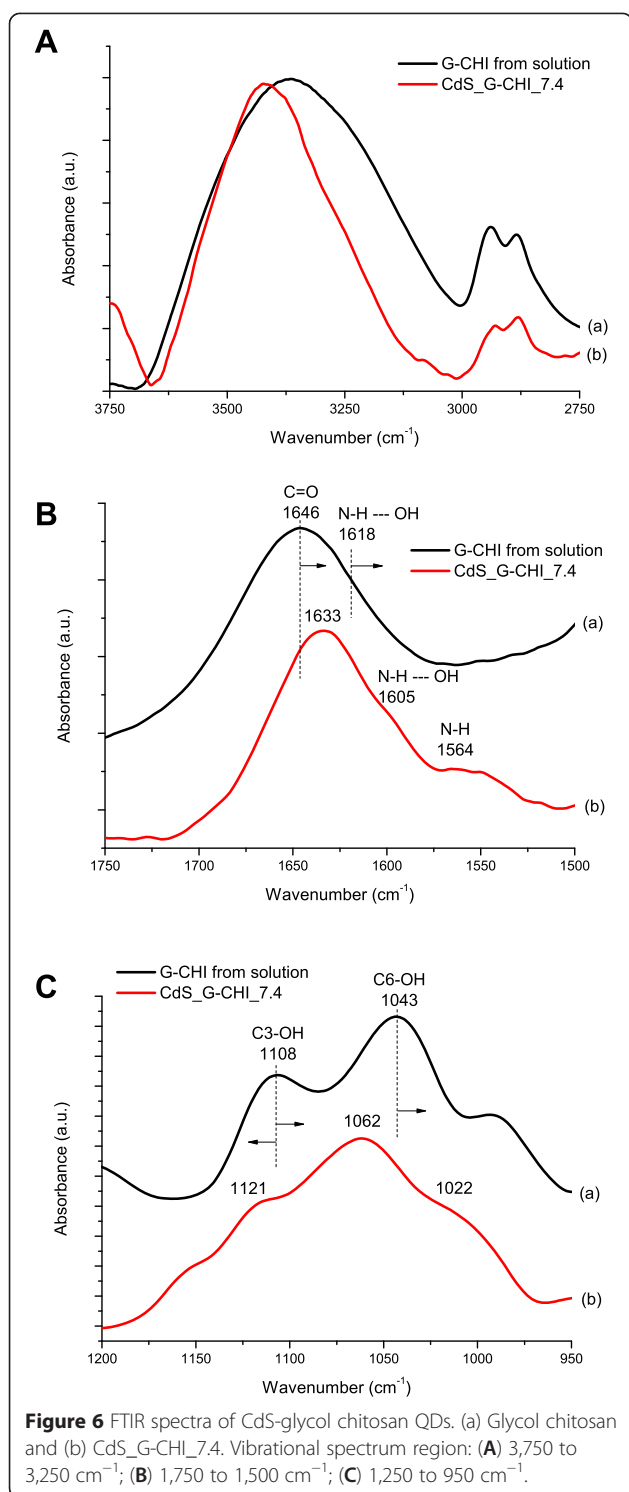


**Figure 5** FTIR spectra of ligands. (a) Glycol chitosan as-supplied. (b) Glycol chitosan in solution (pH =  $7.4 \pm 0.2$ ). (c) Chitosan in solution (pH =  $6.0 \pm 0.2$ ).



primarily attributed to the interactions occurring between the functional groups of the glycol chitosan ligand (amine/acetamide and hydroxyls) and the CdS QDs. The band of glycol chitosan at 3,400 to 3,200  $\text{cm}^{-1}$  region (Figure 6A(a)), corresponding to the stretching vibration of the  $\text{NH}_2$  and OH groups, became significantly

narrower after stabilisation of the CdS quantum dots (Figure 6A(b)). This peak narrowing indicates the reduction of 'free' amine groups after quantum dot stabilisation [40]. Additionally, in the FTIR spectrum of the G-CHI (Figure 6B(a)), the amide I band (at 1,646  $\text{cm}^{-1}$ ) shifted to a lower wavenumber by 13  $\text{cm}^{-1}$  for the CdS nanoconjugates (Figure 6B(b)). The band associated with the primary alcohol (C6-OH) vibration at 1,108  $\text{cm}^{-1}$  was split into two bands at 1,121 and 1,162  $\text{cm}^{-1}$ , and the peak assigned to the C3-OH (secondary alcohol) stretching shifted its position to a lower wavenumber by 21  $\text{cm}^{-1}$ . In addition, the amine band was 'redshifted' (i.e., shifted to a lower wavenumber/energy) due to QD formation. It is believed that CdS nucleation and growth disrupts the hydrogen bonds  $-\text{NH} \cdots \text{OH}$ . Therefore, the band at 1,618  $\text{cm}^{-1}$  shifted to 1,605  $\text{cm}^{-1}$ , and a band at 1,564  $\text{cm}^{-1}$  related to the primary amine was observed. Based on the FTIR analyses, it was determined that the primary and secondary alcohols, amine, and acetamide (carboxyl) groups in glycol chitosan were involved in the stabilisation of the CdS\_G-CHI nanoconjugates.

## Conclusions

In the present study, it is reported the direct synthesis of CdS QDs bio-functionalised by glycol chitosan using a single-step colloidal process at room temperature in acidic (pH = 5.0), physiological (pH = 7.4), and alkaline (pH = 8.4) aqueous media and compared to chitosan analogous system (pH = 6.0). The results indicated that the average diameter of the CdS nanoparticles using G-CHI ligand was larger at acidic conditions (pH = 5.0,  $2R = 2.7$  nm) than at neutral and alkaline solutions ( $2R = 2.1$  nm at pH = 7.4 and pH = 8.4), predominantly associated with the stabilisation of conjugates by the deprotonation of the amine groups. In addition, the DLS results showed that the hydrodynamic diameters of CdS\_G-CHI\_7.4 and CdS\_CHI\_6.0 were  $40.4 \pm 3.3$  and  $16.6 \pm 0.6$  nm, respectively, attributed to the presence of the hydrophilic glycol groups in the chitosan chain leading to the expansion of the polymeric shell of the nanoconjugates by interactions with water molecules. Furthermore, the ZP results indicated that the colloidal stabilisation of CdS nanoconjugates relied on electrostatic interactions and steric hindrance of the polymer ligands to prevent aggregation or coalescence of the nanoparticles in aqueous solutions. Finally, it was demonstrated the feasibility of synthesising fluorescent CdS QDs in aqueous colloidal dispersions at physiological pH, indicating considerable potential to be used as biomarkers for biomedical and pharmaceutical applications in nanomedicine.

## Competing interests

The authors declare that they have no competing interests.

**Authors' contributions**

HSM carried out the experimental design and analysis and drafted the manuscript. AAPM carried out the synthesis, characterisation, and analysis of QDs and drafted the manuscript. Both authors' read and approved the final manuscript.

**Acknowledgements**

The authors acknowledge the financial support from the CAPES, FAPEMIG, and CNPq. The authors express their gratitude to the staff from the Microscopy Centre/UFMG for TEM analysis.

Received: 30 January 2015 Accepted: 24 March 2015

Published online: 10 April 2015

**References**

- Mansur HS. Quantum dots and nanocomposites. *WIREs Nanomeb Nanobi*. 2010;2:113–29.
- Medintz I, Uyeda EL, Goodman ER, Mattousi H, Goodman ER, Mattousi H. Quantum dot bioconjugates for imaging, labelling and sensing. *Nat Mater*. 2005;4:435–46.
- Brus LE. Electron–electron-hole in small semiconductors crystallites: the size dependence of the lowest excited electronic state. *J Chem Phys*. 1984;80:4403–9.
- Green M. The nature of quantum dot capping ligands. *J Mater Chem*. 2010;20:5797–809.
- Mansur HS, Grieser F, Urquhart RS, Furlong DN. Photoelectrochemical behaviour of Q-state CdS<sub>x</sub>Se<sub>1-x</sub> particles in arachidic acid LB films. *J Chem Soc*. 1995;91:3399–404.
- Mansur HS, Vasconcelos WL, Grieser F, Caruso F. Photoelectrochemical behaviour of CdS Q-state semiconductor particles in 10,12 nonacosadiynoic acid polymer LB film. *J Mater Sci*. 1999;34:5285–91.
- Ekimov AI, Onushchenko AA. Quantum size effect in the optical-spectra of semiconductor micro-crystals. *Sov Phys Semicond*. 1982;16:775–8.
- Efros AL. Interband absorption of light in a semiconductor sphere. *Sov Phys Semicond*. 1982;16:772–5.
- Tan WB, Huang N, Zhang Y. Ultrafine biocompatible chitosan nanoparticles encapsulating multi-coloured quantum dots for bioapplications. *J Colloid Interface Sci*. 2007;310:464–70.
- Drbohlavova J, Adam V, Kizek R, Hubalek J. Quantum dots - characterisation, preparation and usage in biological systems. *Int J Mol Sci*. 2009;10:656–73.
- Henglein A. Photodegradation and fluorescence of colloidal cadmium sulfide in aqueous solution. *Ber Bunsen-Ges Phys Chem*. 1982;86:301–5.
- Murray CD, Norris DJ, Bawendi MG. Synthesis and characterisation of nearly monodisperse CdE (E = sulfur, selenium, tellurium) semiconductor nanocrystallites. *J Am Chem Soc*. 1993;115:8706–15.
- Chen N, He Y, Su Y, Li X, Huang Q, Wang H, et al. The cytotoxicity of cadmium-based quantum dots. *Biomaterials*. 2012;33:1238–44.
- Zhuang J, Zhang X, Wang G, Li D, Yang W, Li T. Synthesis of water-soluble ZnS:Mn<sup>2+</sup> nanocrystals by using mercaptopropionic acid as stabilizer. *J Mater Chem*. 2003;13:1853–7.
- Mansur HS, Mansur AAP, Soriano-Araujo A, Lobato ZIP. Fluorescent nanohybrids based on quantum dot-chitosan-antibody as potential cancer biomarkers. *ACS Appl Mater Interfaces*. 2014;6:11403–12.
- Mansur HS, Mansur AAP. Fluorescent nanohybrids: quantum-dots coupled to polymer-recombinant protein conjugates for the recognition of biological hazards. *J Mater Chem*. 2012;22:9006–18.
- Mansur HS, Mansur AAP, González JC. Synthesis and characterisation of CdS quantum dots with carboxylic-functionalized poly (vinyl alcohol) for bioconjugation. *Polymer*. 2011;52:1045–54.
- Dash M, Chiellini F, Ottenbrite RM, Chiellini E. Chitosan - a versatile semi-synthetic polymer in biomedical applications. *Prog Polym Sci*. 2011;36:981–1014.
- Anthonsen MW, Vårum KM, Smidsrød O. Solution properties of chitosans: conformation and chain stiffness of chitosans with different degrees of N-acetylation. *Carbohydr Polym*. 1993;22:193–201.
- Lin Y, Zhang L, Yao W, Qian H, Ding D, Wu W, et al. Water-soluble chitosan-quantum dot hybrid nanospheres toward bioimaging and biolabeling. *ACS Appl Mater Interfaces*. 2011;3:995–1002.
- Mansur HS, Mansur AAP, Curti E, de Almeida MV. Functionalized-chitosan/ quantum dots nano-hybrids for nanomedicine applications: towards biolabeling and biosorbing phosphate metabolites. *J Mater Chem B*. 2013;1:1696–711.
- Ramanery FP, Mansur AA, Mansur HS. One-step colloidal synthesis of biocompatible water-soluble ZnS quantum dot/chitosan nanoconjugates. *Nanoscale Res Lett*. 2013;8:512.
- Mansur HS, Mansur AAP, Curti E, de Almeida MV. Bioconjugation of quantum-dots with chitosan and N, N, N-trimethyl chitosan. *Carbohydr Polym*. 2012;90:189–96.
- Chang S-Q, Kang B, Dai Y-D, Zhang H-X, Chen D. One-step fabrication of biocompatible chitosan coated ZnS and ZnS:Mn<sup>2+</sup> quantum dots via gamma-radiation route. *Nanoscale Res Lett*. 2011;6:591.
- Casettaria L, Vllasaliu D, Castagnino E, Stolnik S, Howdle S, Illum L. PEGylated chitosan derivatives: synthesis, characterisations and pharmaceutical applications. *Progress Polym Sci*. 2012;37:659–85.
- Sun I-C, Na JH, Jeong SY, Kim D-E, Kwon IC, Choi K, et al. Biocompatible glycol chitosan-coated gold nanoparticles for tumor-targeting CT. *Imaging Pharm Res*. 2014;31:1418–25.
- Kim JH, Kim YS, Park K, Kang E, Lee S, Nam HY, et al. Self-assembled glycol chitosan nanoparticles for the sustained and prolonged delivery of antiangiogenic small peptide drugs in cancer therapy. *Biomaterials*. 2008;29:1920–30.
- Lv Y, Li K, Li Y. Surface modification of quantum dots and magnetic nanoparticles with PEG-conjugated chitosan derivatives for biological applications. *Chem Pap*. 2013;67:1404–13.
- Salgado CL, Mansur AAP, Mansur HS, Monteiro FJM. Fluorescent bionanoprobes based on quantum dot-chitosan-o-phospho-l-serine conjugates for labeling human bone marrow stromal cells. *RSC Adv*. 2014;4:49016–27.
- Sogias IA, Khutoryanskiy VV, Williams AC. Exploring the factors affecting the solubility of chitosan in water. *Macromol Chem Phys*. 2010;211:426–33.
- Weller H, Schmidt HM, Koch U, Fojtik A, Baral S, Henglein A, et al. Photochemistry of colloidal semiconductors. Onset of light absorption as a function of size of extremely small CdS particles. *Chem Phys Lett*. 1986;124:557–60.
- Tauc J, Mentha A. States in the gap. *J Non-Cryst Solids*. 1972;8–10:569–85.
- Skobeveva VM, Smyrnytna VA, Sviridova OI, Struts DA, Tyurin AV. Optical properties of cadmium sulfide nanocrystals obtained by the sol–gel method in gelatin. *J Appl Spectrosc*. 2008;75:576–82.
- Smyrnytna V, Skobeveva V, Malushin N. The nature of emission centers in CdS nanocrystals. *Radiat Meas*. 2007;42:693–6.
- Ramsden JJ, Gratzel M. Photoluminescence of small cadmium sulphide particles. *J Chem Soc, Faraday Trans*. 1984;80:919–33.
- Santos JCC, Mansur AAP, Mansur HS. One-step biofunctionalization of quantum dots with chitosan and n-palmitoyl chitosan for potential biomedical applications. *Molecules*. 2013;18:6550–72.
- Harder P, Grunze M, Dahint R, Whitesides GM, Laibinis PE. Molecular conformation in oligo(ethylene glycol)-terminated self-assembled monolayers on gold and silver surfaces determines their ability to resist protein adsorption. *J Phys Chem B*. 1998;102:426–36.
- Ahmed MK, McLeod MP, Nézivar J, Giuliani AW. Fourier transform infrared and near-infrared spectroscopic methods for the detection of toxic diethylene glycol (DEG) contaminant in glycerin based cough syrup. *Spectroscopy*. 2010;24:601–8.
- Quinones JP, Gothelf KV, Kjems J, Caballero AMH, Schmidt E, Covas CP. Self-assembled nanoparticles of glycol chitosan - ergocalciferol succinate conjugate, for controlled release. *Carbohydr Polym*. 2012;88:1373–7.
- Cooper JK, Franco AM, Gul S, Corrado C, Zhang JZ. Characterisation of primary amine capped CdSe, ZnSe, and ZnS quantum dots by FT-IR: determination of surface bonding interaction and identification of selective desorption. *Langmuir*. 2011;27:8486–93.